Load Noise Prediction of High-Voltage Transformers by Equation Applying 3-D EMCN

DAE-KEE KIM[1], **JUN-YEOL RYU**[1], **DONG-MIN KIM**[1], **DO JIN KIM**[2], **AND MYUNG-SEOP LIM**[1], (Member, IEEE)

[1]Department of Automotive Engineering, Hanyang University, Seoul 04763, South Korea
[2]Power and Industrial Systems Research and Development Center, Hyosung Corporation, Anyang 14080, South Korea

Corresponding author: Myung-Seop Lim (myungseop@hanyang.ac.kr)

ABSTRACT This paper proposes a method for predicting the load noise of high-voltage (HV) transformers. When the transformer is loaded, the electromagnetic force is generated by the interaction between electric and magnetic fields. This force, the so-called Lorentz force, induces the vibration of the winding structure causing the load noise of transformer. Therefore, calculating the Lorentz force plays a crucial role in predicting the load noise. Herein, a 3-Dimensional equivalent magnetic circuit network (3-D EMCN) is applied to calculate the Lorentz force, instead of 3-Dimensional finite element analysis (3-D FEA) to shorten the computation time. Subsequently, considering the relationship between the sound pressure and the Lorentz force, the calculated force can be applied in the equation for the sound pressure level (SPL), which represents the relative sound pressure on a logarithmic scale. The formula for the sound pressure varies depending on the sound source model. The source model of load noise can be represented as a dipole source because the structure of the transformer windings is considered as an unbaffled speaker. The transformer parameters identified to affect the load noise are additionally considered for more accurate prediction of load noise. The parameters identified to increase the load noise are simply multiplied to the equation, whereas those with the opposite effect are multiplied inversely. Finally, after this compensation process, the accuracy of the load noise prediction equation is calculated as the standard deviation of the differences between the experimental and calculated results.

INDEX TERMS 3-D EMCN, load noise, Lorentz force, sound pressure level, transformer.

I. INTRODUCTION

The rapid growth of the entire industry and recent interest in sustainable development have increased the requirements for electrical power supplies and demand for high-voltage (HV) transformers. Furthermore, noise regulations have been established owing to the increasing interest in improving the quality of life. The noise generated by HV transformers should be predicted to satisfy these standards in the design process [1].

There are several kinds of transformer noise; load noise, caused by the electromagnetic force generated by the interaction between electric and magnetic fields; core noise, produced by magnetostriction of the laminated core; cooling noise, generated by the cooling components of transformers such as cooling fans. Among these noise sources, load noise

The associate editor coordinating the review of this manuscript and approving it for publication was Flavia Grassi.

becomes the dominant source of total transformer noise with an increase in the transformer power [2]–[4].

Previous studies on the noise generated by transformers are as follows: The effect of harmonic loads on the audible noise of transformers was analyzed in [5]. This study showed the relationship between total harmonic distortion (THD) and the change in load noise but did not predict the load noise. On the other hand, electromagnetic, structural, and acoustic analyses of noise, considering the windings and cores of transformers are shown in [6], [7] by applying 3-Dimensional finite element analysis (3-D FEA). This method may provide accurate predictions of load noise, but it is difficult to expect results in a short time because its pre-processing and computing times are relatively long. Reference [8], [9] focused on core noise whereas the transformer noise was measured and analyzed, using the sound intensity method in [10]. R.Girgis *et al.* determined some causes of the differences between on-site and factory measured noise [11]

and predicted the noise of the transformer considering core resonance [12].

For designers, it is helpful to predict load noise of transformer before construction, especially during the initial design process. To predict the load noise of various transformer models, it is desirable to use an analytical equation, as the computing time for prediction can be reduced compared with that of FEA. In addition, the parameters that contribute to noise generation can be identified while deriving the load noise prediction equation.

Thus, this paper deals with the process of derivation of an equation, that predicts the load noise of HV transformers. First, the electromagnetic force, the so-called Lorentz force which is the main source of load noise is calculated. A 3-Dimensional equivalent magnetic circuit network (3-D EMCN) is applied for this calculation process, resulting in reductions of computing and pre-processing time. Subsequently, because the sound pressure is generated when the Lorentz force causes the vibration of the transformer windings, resulting in load noise, the calculated Lorentz force is applied to the equation of the sound pressure level (SPL) to express the relationship between the Lorentz force and load noise. The structure of the windings and legs of the transformer core is simplified to an unbaffled speaker, which can be described as a dipole sound source model. This determines the form of the sound pressure equation and provides the basis for predicting the transformer load noise. In addition, to improve the accuracy of equation for predicting load noise, additional transformer parameters that are identified to affect the load noise are considered. Parameters confirmed to increase the load noise are directly multiplied to the equation, while those with the opposite effect are inversely multiplied. The accuracy of the load noise prediction equation is calculated as the standard deviation of the differences between the measured and calculated results. The load noise levels from 32 transformers are measured experimentally. Finally, to verify the accuracy of the equation, the measured load noise results from the additional transformers are compared with the predicted results. Fig. 1 shows the overall process of load noise prediction generated by HV transformers. The contributions of this study are as follows:

- The computation time of load noise transformers can be reduced using the proposed method.
- The load noise of transformers can be predicted accurately within a standard deviation of 1.9 dBA.
- The prediction equation suggested by this study can be applied in the design process of transformers.

II. COMPUTATION OF THE LORENTZ FORCE WITH 3-D EMCN

Noise is an unwanted sound produced by vibrating objects excited by external forces. Therefore, the characteristics of the forces and the object are necessary to predict the noise. First, this section focuses on calculating the Lorentz force that is generated by the transformer windings and acts on each winding.

A. INTRODUCTION TO 3-D EMCN

The active part of the transformer where the Lorentz force is primarily generated is shown in Fig.2. The high- and low-voltage windings are wound on the legs which are the vertical parts of the steel core. The yokes are the horizontal parts of the steel core.
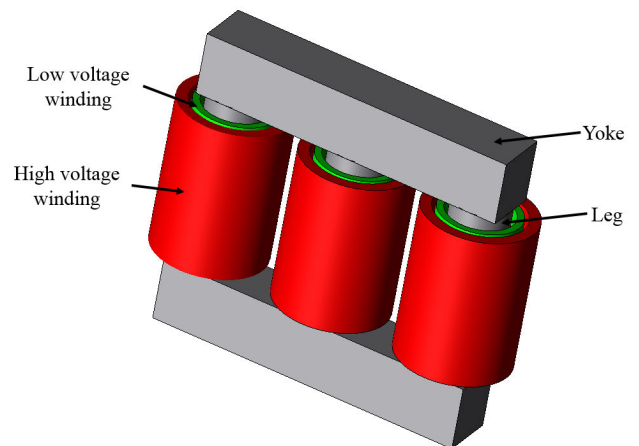

FIGURE 2. Simplified structure of the active part of the transformer.

However, the computational time for calculating Lorentz force of the transformer by 3-D FEA is relatively long. In addition, because the geometric parameters and power conditions vary with each transformer model, pre-processing for analyzing each model by 3-D FEA can be troublesome. In this study, to address these shortcomings, 3-D EMCN is applied for the computation process. The active part of the transformer model shown in Fig. 2 can be divided into small elements as shown in the top right of Fig. 3. Subsequently, the nodes of the EMCN shown in the bottom right of Fig. 3 are applied to those elements assuming that all the nodes are located at the center of the elements. As a result, each element of this network can be represented as circuit parameters thereby formulating the entire 3-D transformer model by 3-D EMCN, as shown in the bottom left of Fig. 3. The Lorentz forces generated by loaded transformer are calculated by
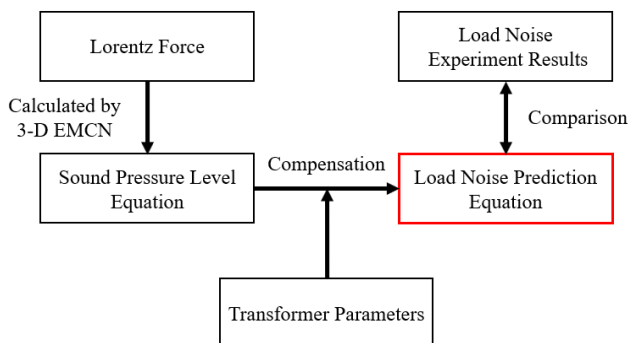

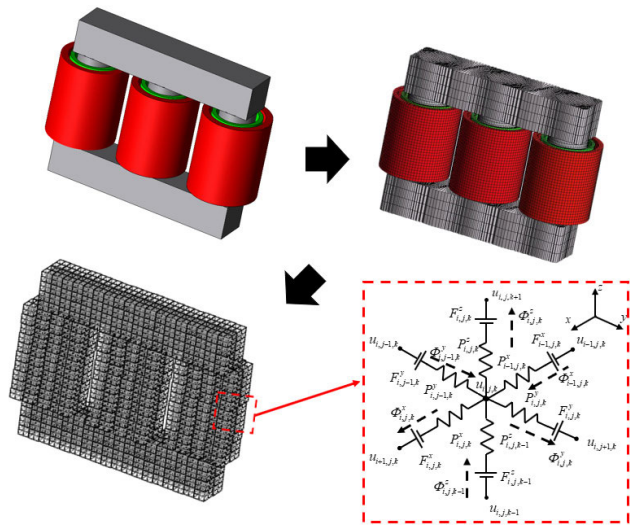**FIGURE 1.** The block diagram of overall process of load noise prediction.

FIGURE 3. Formulation process of the entire active part of transformer using 3-D EMCN and the arbitrary node of 3-D EMCN.

solving equation derived from nodes of 3-D EMCN. As mentioned above, arbitrary nodes in 3-D EMCN is shown in right bottom of Fig. 3 using a Cartesian coordinate system, where u is the unknown magnetic scalar potential; the superscripts x, y, and z denote the directions of the Cartesian coordinate system, and the subscripts i, j, and k denote the corresponding node position indexes. P is the permeance, which is calculated using the geometry; F is the magnetomotive force; Φ with a dashed line indicates the magnetic flux between two adjacent nodes. The equations for each arbitrary element can be represented by (1) and (2), using Gauss's law and the magnetic circuit equations between two nodes [13].

$$\Phi_{i-1,j,k}^{x} + \Phi_{i,j-1,k-1}^{y} + \Phi_{i,j,k-1}^{z} - \Phi_{i,j,k}^{x}$$
$$-\Phi_{i,j,k}^{y} - \Phi_{i,j,k}^{z} = 0 \quad (1)$$

$$\begin{cases} \Phi_{i-1,j,k}^{x} = P_{i-1,j,k}^{x}\left(u_{i-1,j,k} - u_{i,j,k} + F_{i-1,j,k}^{x}\right) \\ \Phi_{i,j,k}^{x} = P_{i,j,k}^{x}\left(u_{i,j,k} - u_{i+1,j,k} + F_{i,j,k}^{x}\right) \\ \Phi_{i-1,j,k}^{x} = P_{i-1,j,k}^{x}\left(u_{i-1,j,k} - u_{i,j,k} + F_{i-1,j,k}^{x}\right) \\ \Phi_{i,j,k}^{x} = P_{i,j,k}^{x}\left(u_{i,j,k} - u_{i+1,j,k} + F_{i,j,k}^{x}\right) \\ \Phi_{i-1,j,k}^{x} = P_{i-1,j,k}^{x}\left(u_{i-1,j,k} - u_{i,j,k} + F_{i-1,j,k}^{x}\right) \\ \Phi_{i,j,k}^{x} = P_{i,j,k}^{x}\left(u_{i,j,k} - u_{i+1,j,k} + F_{i,j,k}^{x}\right) \end{cases} \quad (2)$$

The above equation is represented as $\boldsymbol{P} \bullet \boldsymbol{u} = \boldsymbol{D}$, where $\boldsymbol{P}$ is the permeance matrix, $\boldsymbol{u}$ is the potential matrix, and $\boldsymbol{D}$ is the driving matrix. Thus, the magnetic scalar potential is obtained by solving this simple equation. Then, the magnetic flux density of each element can be calculated using the scalar potential.

B. CALCULATION AND VERIFICATION OF LORENTZ FORCE USING 3-D EMCN

The 3-D EMCN shortens the computing time with simple equations and also makes pre-processing easier than

3-D FEA. The accuracy of the 3-D EMCN is important for accurate predictions of the load noise of HV transformers. This can be verified by comparing the calculation results of the 3-D EMCN for the Lorentz force with those of 3-D FEA under the same load conditions. Grain-oriented steel is commonly used to enhance transformer performance [14], [15]. Thus, the relative permeabilities in each direction (i.e., the x, y, and z directions) are different. Fig. 4 shows that the magnetic flux density for this transformer model obtained through nonlinear analysis is 0.52 T.

The logarithmic form of the B–H curve for the transformer core is shown in Fig. 5. The easy direction is the grain-oriented direction, as mentioned above, and the others are hard directions. The easy direction is determined by the direction of the magnetic flux. The calculation results indicate that the range of the magnetic flux density is in the linear region of Fig. 5. Thus, the relative permeability of the transformer core can be applied as a constant value that enables linear analysis. Fig. 6 shows the electromagnetic phenomenon when currents are applied to both the high- and low-voltage coils of the transformer. The green and red dashed lines represents
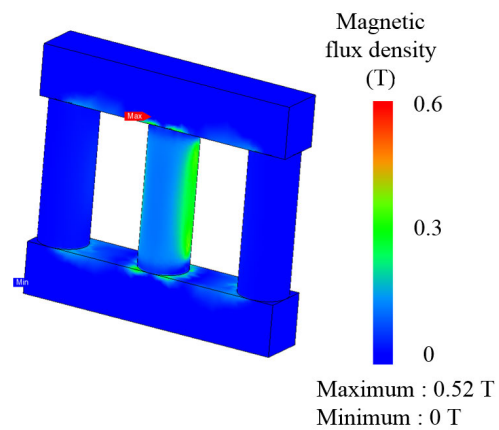

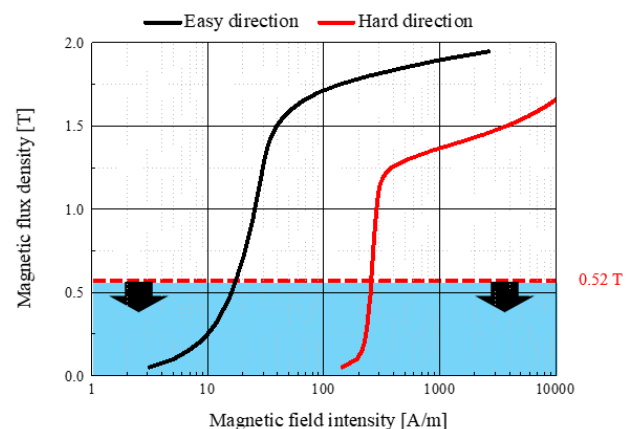**FIGURE 4.** Nonlinear analysis result of magnetic flux densities using 3-D FEA.

FIGURE 5. Logarithmic form of B–H curve for the transformer core.

the magnetomotive forces of the low- and high-voltage coils, respectively. Currents are applied to the coils in opposite directions under load conditions. Therefore, the magnetic flux densities in the regions inside the low-voltage coil and outside the high-voltage coil are zero. The force density is calculated using (3), where **J** is the current density, **B** is the flux density, and **f** is the force density of the coil. In Fig. 6, the directions of the current, flux density, and force density are presented.
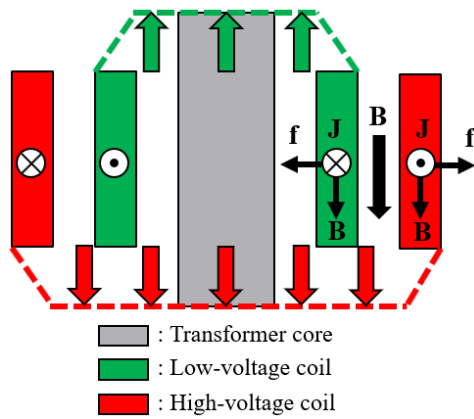
$$\mathbf{J} \times \mathbf{B} = \mathbf{f} \tag{3}$$

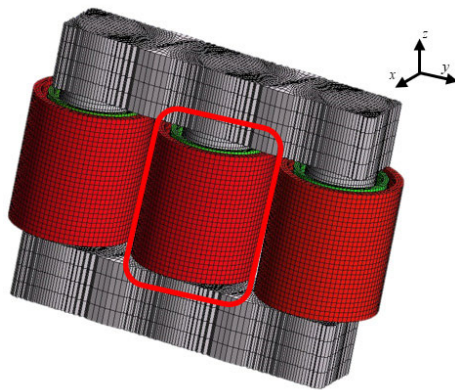**FIGURE 6.** Lorentz forces of the low and high-voltage coils.

FIGURE 7. 3-D 3-phase transformer model using 3-D EMCN.

Fig. 7 shows the 3-D 3-phase transformer model obtained using the 3-D EMCN. The Lorentz force densities are calculated around the circumference of the middle part of the winding, which is in the middle leg of the transformer model. The red square in Fig. 7 denotes this region. A comparison of the Lorentz force densities calculated using the 3-D EMCN and 3-D FEA is shown in Fig. 8. The radial component of the Lorentz force density is compared. The black line with round symbols indicates the 3-D EMCN result and the red line indicates the 3-D FEA result. The normalized root-mean-square error (NRMSE) between the two results is 2.6%, and
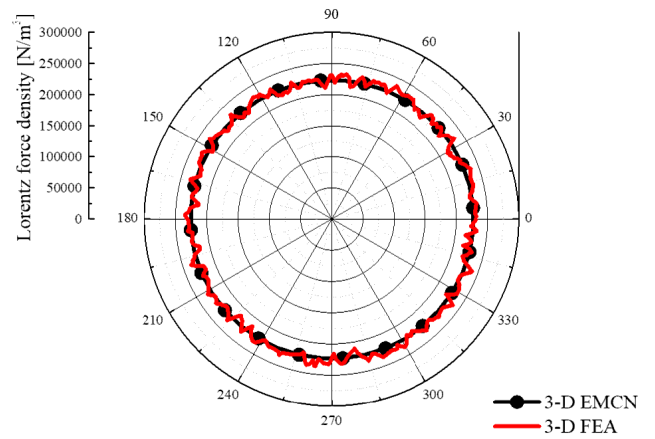

FIGURE 8. Comparison of Lorentz force densities calculated using the 3-D EMCN and 3-D FEA.

the computing time for the 3-D EMCN was approximately 1 min, while that of 3-D FEA was about 30 min. The results for the computation time are listed in Table 1.

TABLE 1. Computation time for Lorentz force calculation using different methods.

Computation method	Computation time
3-D EMCN	1 min
FEA	30 min

Thus, the 3-D EMCN shortens the computing time while maintaining the calculation accuracy. The 3-D EMCN is applied to calculate the Lorentz force to predict the load noise of a 3-phase HV transformer in Section III.

III. APPLICATION OF THE LORENTZ FORCE TO THE SPL EQUATION

The Lorentz force generated by the transformer induces the vibration of the winding structure. This vibration causes acoustic propagation, thereby generating load noise. Thus, to predict the load noise, the relationship between the Lorentz force and sound pressure should be considered by using equations. In this section, the definition of SPL is discussed. After the appropriate form of the sound pressure that can be applied to the structure of the transformer is obtained, the relationship between the Lorentz force and the SPL will be shown as an initial load noise prediction equation.

A. EXPRESSION OF SPL
The SPL can be expressed as (4), where P_{rms} is the root-mean-square (RMS) value of the sound pressure and P_{ref} represents the reference sound pressure, whose value is generally 20 μPa. The unit of the SPL is decibels [16].

$$\text{SPL} = 10\log_{10}\left(\frac{P_{rms}^2}{P_{ref}^2}\right) \tag{4}$$
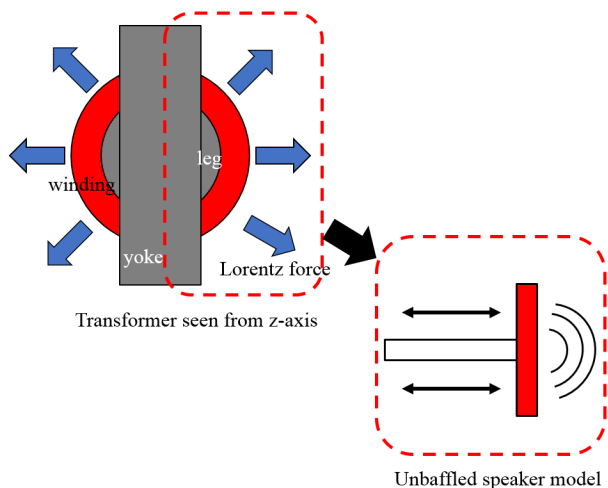
FIGURE 9. Simplified transformer model and unbaffled speaker model.

Thus, it is important to investigate the relationship between the sound pressure and Lorentz force generated by the windings to predict the load noise of a 3-phase transformer.

The formula for the sound pressure varies depending on the noise source model. Fig. 9 shows a simplified model of the transformer core and windings viewed from the *z*-axis. The gray and red area indicates the core and winding, respectively. The radial component of the Lorentz force acts on the winding and causes it to fluctuate, generating load noise. This mechanism is similar to that of a speaker. Thus, half of the simplified model can be viewed as an unbaffled speaker. An unbaffled speaker can be described as a dipole source model. The RMS amplitude of the sound pressure of a dipole model is shown in (5), where *c* is the speed of the sound wave, which is approximately 340 m/s; *K* is the wavenumber, which represents the rate of change of phase with the position; ρ_0 is the air density; *r* is the distance from the sources; *s* is the distance between the two sources. *Q* is the monopole source strength, which can be represented as (6) and is the surface integral of the dot product of the normal vector for the surface **n** and the particle velocity vector **v** [16].

$$P_{rms} = \frac{\left(\rho_0 c K^2 Q s\right)}{\sqrt{2}\,(4\pi r)} \tag{5}$$

$$Q = \int_S \mathbf{v} \cdot \mathbf{n}\, dS \tag{6}$$

B. APPLICATION OF THE LORENTZ FORCE
Equation (6) can be calculated as (7), where *A* is the surface area of the winding and *v* is the amplitude of the particle velocity.

$$Q = Av \tag{7}$$

The surface area can be obtained easily using the geometrical information of the winding. The amplitude of the particle velocity can be assumed as the pulsation speed of the

winding. A forced response by harmonic excitation can be applied in this situation because the Lorentz force acts as an excitation force for pulsating the winding. Thus, the pulsation speed of a vibrating object can be expressed as (8), where F_0 is the magnitude of the Lorentz force, *k* is the winding stiffness, ω is the frequency of the force, and *m* is the mass of the winding.

$$v = \frac{F_0}{k - m\omega^2} \tag{8}$$

Subsequently, the winding stiffness can be represented using the coil parameters. Considering the winding structure as a finite-length cylinder, a simplified form of the stiffness can be represented as (9), where *D* is the diameter of the winding and *E* is the modulus of elasticity. *I* is the moment of inertia, represented as (10), where *d* is the winding thickness, and L_c is the winding height [17].

$$k \propto \frac{16\pi EI}{D^3} \tag{9}$$

$$I = \frac{d^3 L_c}{12} \tag{10}$$

By using equations (5)–(10), the initial equation for the sound pressure is shown as (11). The initial form of the load noise prediction equation is obtained by (12) by applying (11) to (4).

$$P_{rms} = \frac{\left(\rho_0 c K^2 A s\right)}{\sqrt{2}\,(4\pi r)} \frac{12 D^3 F_0}{16\pi E d^3 L_c - 12 D^3 m\omega^2} \tag{11}$$

$$Noise = 20\log_{10}\left(\frac{12 D^3 \rho_0 c K^2 A F_0 s}{\left(16\pi E d^3 L_c - 12 D^3 m\omega^2\right) 4\sqrt{2}\pi r P_{ref}}\right) \tag{12}$$

Thus, the Lorentz force calculated using the 3D-EMCN, can be applied to the SPL equation. As the Lorentz force can be calculated within 1 min, the load noises of various transformer models can be quickly obtained. The accuracy of this prediction equation will be calculated in the following section.

IV. COMPENSATION AND VERIFICATION OF THE PREDICTION EQUATION FOR LOAD NOISE
As the load noise prediction equation has been derived, it is important to determine how the equation can accurately predict the load noise of an HV transformer. Moreover, as mentioned in Fig. 1 and Section II, the characteristics of the object play significant roles in generating noise and vibration. Thus, applying the characteristics of HV transformers can increase the accuracy of the equation. In this section, modifications by adding some design parameters of the transformer and the verification of the load noise prediction equation are discussed.

A. COMPENSATION OF THE LOAD NOISE PREDICTION EQUATION
As noise is generated when forces act on the structure of the object, the transformer properties related to their structures

should be applied to the initial equation for obtaining a more accurate noise prediction equation. Several parameters that are considered to affect the noise generation are added to the equation.

The thickness of the windings and insulating paper may affect the SPL. The winding thickness can be considered to reduce the load noise by increasing the stiffness considering (9) and (10). On the other hand, because the winding is the main source of the Lorentz force, which is the primary cause of load noise, the winding thickness can also be considered as a parameter increasing the noise. The insulation paper does not participate in generating the Lorentz force. It acts as a bridge to transmit the vibration between the conductors of the transformer winding and can be modeled as a spring and damper in the transformer winding model, as shown in Fig. 10 (a) [18], [19]. Thus, the thickness of the insulation paper can be considered as an additional parameter for an improved equation. A thicker insulation paper may reduce the load noise by cushioning the vibration between the conductors of the windings. The area of the tank wall is also an important factor because the load noise generated from the active part of the transformer inside the tank is transmitted to the tank wall of the transformer, as shown in Fig. 10 (b), and the load noise is measured at the outside of the tank wall [20], [21]. Thus, the tank width of the transformer should

be multiplied to the initial equation, while the thickness of the insulation paper should be inversely multiplied. The winding thickness, which has both increasing and decreasing effects on the load noise, should simply be multiplied and its effect on load noise is determined by weight factors. The modified equation is shown in (13), where x, y, and z indicate the weight factors of each parameter obtained by the fitting; T_s is the tank width; d is the winding thickness, and t is the thickness of the insulating paper. The weight factors x, y, and z are determined by applying generalized reduced gradient (GRG) nonlinear method to minimize the standard deviation of the differences between the experimental and calculated results.

$$Noise = a \log_{10}\left(\frac{d^x}{t^y}(T_s)^z \times \frac{ck^2 AF_0 s}{mr}\right) + b \quad (13)$$

B. VERIFICATION OF LOAD NOISE PREDICTION EQUATIONS

Experiments for assessing the load noise for several models of HV transformers are necessary to evaluate the accuracy of the noise prediction equation. Fig. 11 shows one of the of HV transformers are necessary to evaluate the accuracy of the noise prediction equation. Fig. 11 shows one of the transformer models whose capacity is 105 MVA. The load noise is measured around the transformer, as shown in Fig. 12. The mean value for each measurement point is assumed to be the experimental load noise of the transformer. The load noise results obtained via the experiment are compared with the load noise calculated using the initial and improved equations in Fig. 13. The standard deviation of the differences between the experimental and calculated results is determined to verify the accuracy of the equations. Smaller differences indicate that the equation predicts the load noise more accurately. The load noise levels from 32 different transformers were compared with the load noise levels calculated using (12) and (13). The results are shown in Fig. 14.
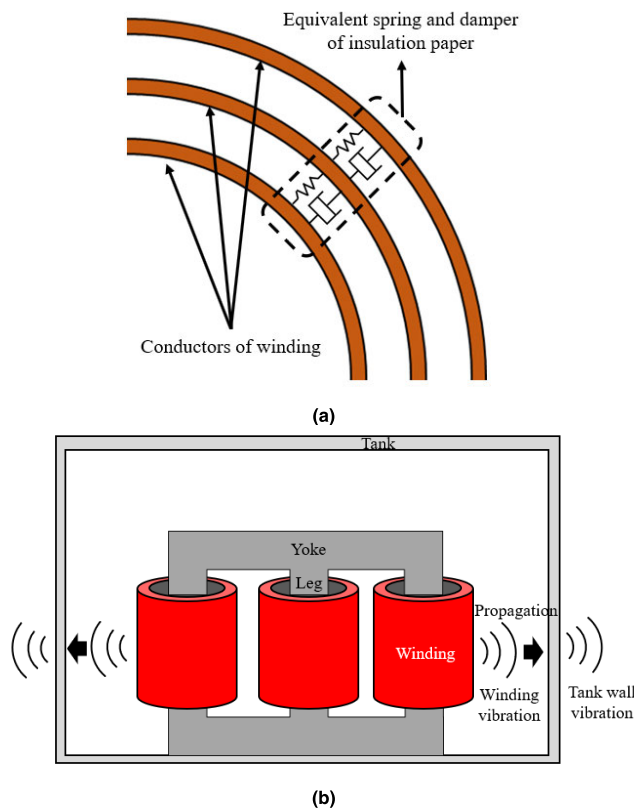

FIGURE 10. (a) Insulation paper modeled as an equivalent spring and damper in the winding structure. (b) Propagation of winding vibration to the tank wall of the transformer.

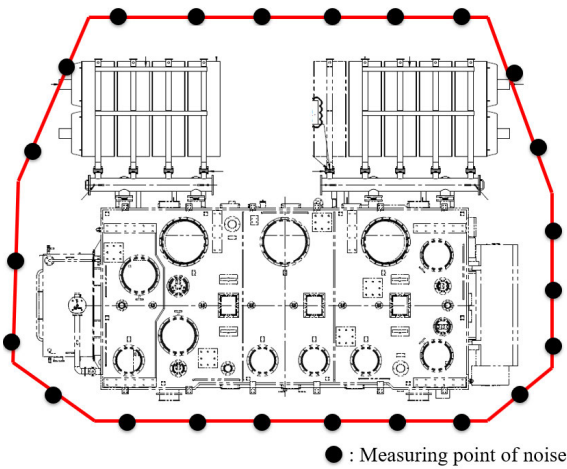**FIGURE 11.** 105 MVA HV transformer for measuring load noise.

: Measuring point of noise

FIGURE 12. Measurement points for the load noise of an HV transformer.
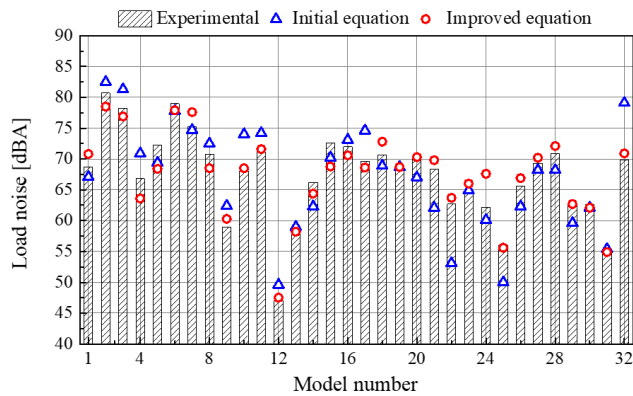

FIGURE 13. Comparison of load noise results obtained via experiment and prediction equations.
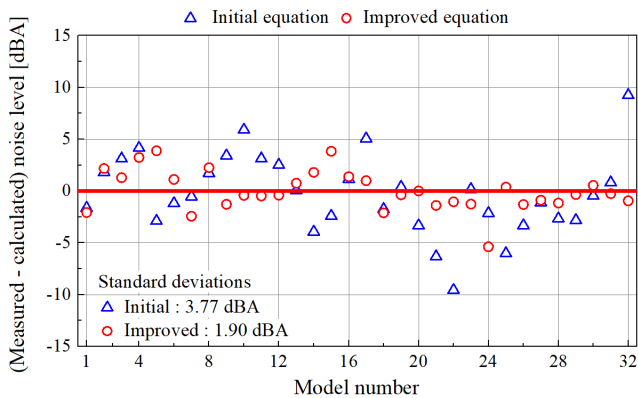

FIGURE 14. Difference of load noise between experimental and prediction results.

The voltage of the transformers used ranges from 110 to 220 kV, whereas the capacity ranges from 100 to 200 MVA. Each point indicates the difference between the measured and calculated noise levels. The accuracy increases when the difference value approaches zero. The standard deviation of the difference obtained using the initial prediction equation is

TABLE 2. Experimental and calculated results of load noise for HV transformers.

Model number	Experimental load noise (dBA)	Calculated load noise by initial equation (dBA)	Calculated load noise by improved equation (dBA)
1	68.7	67.1	70.8
2	80.7	82.5	78.5
3	78.2	81.3	76.9
4	66.8	70.9	63.6
5	72.3	69.4	68.4
6	79.0	77.8	77.9
7	75.2	74.7	77.6
8	70.8	72.5	68.5
9	59.0	62.4	60.3
10	68.1	74.0	68.5
11	71.1	74.2	71.6
12	47.1	49.6	47.5
13	58.9	59.0	58.2
14	66.2	62.3	64.4
15	72.6	70.2	68.8
16	72.0	73.1	70.6
17	69.6	74.6	68.6
18	70.7	68.9	72.8
19	68.3	68.7	68.7
20	70.3	67.0	70.3
21	68.4	62.1	69.8
22	62.7	53.1	63.7
23	64.7	64.9	66.0
24	62.2	60.1	67.6
25	56.0	50.0	55.6
26	65.6	62.3	66.9
27	69.3	68.2	70.2
28	70.9	68.2	72.1
29	62.4	59.6	62.7
30	62.6	62.1	62.1
31	54.6	55.4	54.9
32	69.9	79.1	70.9

3.77 dBA, whereas that obtained using the improved equation is 1.90 dBA, showing a reduction of 1.87 dBA. Considering the features of the forces and object, predicting the load noise using the improved equation is more accurate. The experimental and calculated results of the load noise for all the HV transformer models are listed in Table 2. Moreover, three additional transformer models are considered to verify the accuracy of the improved equation for predicting the load noise of the transformers. These models are different from the 32 models listed in Table 2. The load noise levels of these three additional transformers were measured via experiment
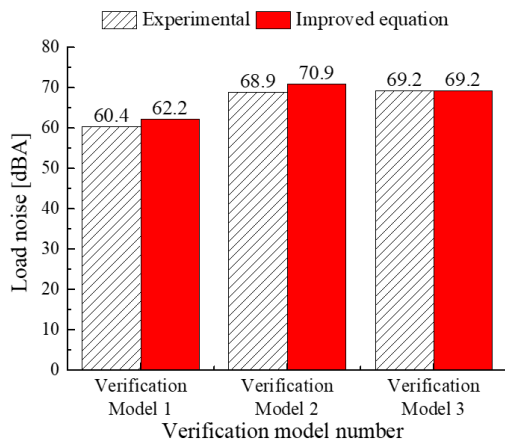
FIGURE 15. Verification of improved load noise prediction equation.

and these results were compared with the load noise calculated using the improved prediction equation. The differences between the measured and calculated noise levels of the additional transformers are 1.8, 2.0, and 0 dBA. This indicates that the improved equation can accurately predict the load noise of HV transformers. The result is shown in Fig. 15.

V. CONCLUSIONS

This paper presented a prediction process for the load noise of HV transformers. A 3-D EMCN was used to calculate the Lorentz force, which is the main source of load noise. The proposed computation method reduced the computing time by 29 min and shortened the pre-processing time compared with that of the 3-D FEA. The linear analysis was possible because of the low magnetic flux density (0.52 T) of the core. The accuracy of the initial equation for applying the calculated electromagnetic force to the SPL was calculated as the standard deviation of the differences between the measured and calculated load noises, i.e., 3.77 dBA. After the modification, the standard deviation was reduced by 1.87 dBA, yielding an improved value of 1.9 dBA. Furthermore, the measured load noises of additional transformers were compared with the calculated load noise for accuracy verification. The standard deviation decreased to 1.87 dBA, which indicates that this equation can accurately predict the load noise of HV transformers. This study can help designers predict the load noise of HV transformers before construction.

REFERENCES

[1] A. Imdadullah, S. M. Amrr, M. S. Jamil Asghar, I. Ashraf, and M. Meraj, "A comprehensive review of power flow controllers in interconnected power system networks," *IEEE Access*, vol. 8, pp. 18036–18063, 2020.

[2] L. F. Braña, C. M. A. Vasques, H. M. R. Campelo, and X. M. Lopez-Fernandez, "Quiet transformers: Design issues," presented at the Adv. Res. Workshop Transformers, Baiona, Spain, Oct. 30, 2013.

[3] L. Lukic, M. Djapic, D. Lukic, and A. Petrovic, "Aspects of design of power transformers for noise reduction," in *Proc. 4th Int. Conf. Noise Vib.*, Niš, Serbia, Oct. 2012, p. 10.

[4] A. Secic, M. Krpan, and I. Kuzle, "Vibro-acoustic methods in the condition assessment of power transformers: A survey," *IEEE Access*, vol. 7, pp. 83915–83931, 2019.

[5] M. Ertl and S. Voss, "The role of load harmonics in audible noise of electrical transformers," *J. Sound Vib.*, vol. 333, no. 8, pp. 2253–2270, Apr. 2014.

[6] H. Jingzhu, Y. Yang, L. Qingfen, L. Dichen, and L. Shanshan, "Electromagnetic vibration noise analysis of transformer windings and core," *IET Electr. Power Appl.*, vol. 10, no. 4, pp. 251–257, Apr. 2016.

[7] K. Bouayed, L. Mebarek, V. Lanfranchi, J.-D. Chazot, R. Marechal, and M.-A. Hamdi, "Noise and vibration of a power transformer under an electrical excitation," *Appl. Acoust.*, vol. 128, pp. 64–70, Dec. 2017.

[8] M. Mizokami and Y. Kurosaki, "Noise variation by compressive stress on the model core of power transformers," *J. Magn. Magn. Mater.*, vol. 381, pp. 208–214, May 2015.

[9] G. Shilyashki, H. Pfützner, P. Hamberger, M. Aigner, A. Kenov, and I. Matkovic, "Spatial distributions of magnetostriction, displacements and noise generation of model transformer cores," *Int. J. Mech. Sci.*, vol. 118, pp. 188–194, Nov. 2016.

[10] Z. Lu, C. Zhang, T. Wang, H. Yu, Z. Wang, C. Li, and G. Liu, "Measurement and analysis of UHV transformer noise with sound intensity and vibration method," in *Proc. 20th Int. Conf. Electr. Mach. Syst. (ICEMS)*, Sydney, NSW, Australia, Aug. 2017, pp. 1–4.

[11] R. Girgis and M. Bernesjö, "Contributions to differences between on-site and factory-measured noise levels of power transformers," *IEEE Trans. Power Del.*, vol. 30, no. 1, pp. 82–88, Feb. 2015.

[12] R. S. Girgis, M. S. Bernesjö, S. Thomas, J. Anger, D. Chu, and H. R. Moore, "Development of Ultra-Low-Noise transformer technology," *IEEE Trans. Power Del.*, vol. 26, no. 1, pp. 228–234, Jan. 2011.

[13] J. H. Sim, D. G. Ahn, D. Y. Kim, and J. P. Hong, "3-D equivalent magnetic circuit network method for precise and fast analysis of PM-assisted claw-pole synchronous motor," *IEEE Trans. Ind. Appl.*, vol. 54, no. 1, pp. 228–234, Feb. 2018.

[14] S. Takajo, T. Ito, T. Omura, and S. Okabe, "Loss and noise analysis of transformer ComprisingGrooved grain-oriented silicon steel," *IEEE Trans. Magn.*, vol. 53, no. 9, Sep. 2017, Art. no. 2001606.

[15] I. Žiger, B. Trkulja, and Ž. Štih, "Determination of core losses in open-core power voltage transformers," *IEEE Access*, vol. 6, pp. 29426–29435, 2018.

[16] D. A. Bies, and C. H. Hansen, *Engineering Noise Control: Theory and Practice*. Boca Raton, FL, USA: CRC Press, 2017, pp. 36–181.

[17] J. F. Gieras, C. Wang, and J. C. Lai, "Stator system vibration analysis," in *Noise Polyphase Electric Motors*. Boca Raton, FL, USA: CRC Press, 2005, pp. 107–115.

[18] M. Jin and J. Pan, "Effects of insulation paper ageing on the vibration characteristics of a transformer winding disk," *IEEE Trans. Dielectr. Electr. Insul.*, vol. 22, no. 6, pp. 3560–3566, Dec. 2015.

[19] H. Zhou, K. Hong, H. Huang, and J. Zhou, "Transformer winding fault detection by vibration analysis methods," *Appl. Acoust.*, vol. 114, no. 15, pp. 136–146, Dec. 2016.

[20] B. García, J. C. Burgos, and M. Alonso, "Transformer tank vibration modeling as a method of detecting winding deformations—Part I: Theoretical foundation," *IEEE. Trans. Power Del.*, vol. 21, no. 1, pp. 157–163, Dec. 2005.

[21] M. Jin and J. Pan, "Vibration transmission from internal structures to the tank of an oil-filled power transformer," *Appl. Acoust.*, vol. 113, no. 1, pp. 1–6, Dec. 2016.

DAE-KEE KIM received the bachelor's degree in mechanical engineering from Hanyang University, Seoul, South Korea, in 2014, where he is currently pursuing the Ph.D. degree in automotive engineering.

His research interests include design and optimization of electric machines and analysis of vibration generated by electric machines.

JUN-YEOL RYU received the bachelor's degree in mechanical engineering and electronic systems engineering from Hanyang University, Ansan, South Korea, in 2016. He is currently pursuing the Ph.D. degree in automotive engineering with Hanyang University, Seoul, South Korea.

His research interests include design and optimization of electric machines and analysis of electro-magnetic field.

DO JIN KIM received the bachelor's degree in electrical engineering from Changwon National University, Changwon, South Korea, in 2011, and the master's and Ph.D. degrees in automotive engineering from Hanyang University, Seoul, South Korea, in 2009 and 2014, respectively.

Since 2014, he has been a Principal Researcher with Hyosung Corporation. His research interests include electromagnetic field analysis and electric machinery for industrial applications.

DONG-MIN KIM received the B.S. degree in electronic information systems engineering from Hanyang University, Ansan, South Korea, in 2013. He is currently pursuing the Ph.D. degree in automotive engineering with Hanyang University, Seoul, South Korea.

His research interests include design of electric machines for automotive and industrial applications and modeling of electric vehicles and hybrid electric vehicles.

MYUNG-SEOP LIM (Member, IEEE) received the bachelor's degree in mechanical engineering and the master's and Ph.D. degrees in automotive engineering from Hanyang University, Seoul, South Korea, in 2012, 2014, and 2017, respectively. From 2017 to 2018, he was a Research Engineer with Hyundai Mobis, Yongin, South Korea. He was an Assistant Professor with Yeungnam University, Daegu, South Korea, in 2018. Since 2019, he has been with Hanyang University, where he is currently an Assistant Professor. His research interests include electro-magnetic field analysis and the design of electric machinery for mechatronics systems, such as automobiles and robotics.

• • •